THE EFFECT OF FILM COMPOSITION ON THE TEXTURE AND GRAIN SIZE OF CuInS$_2$ PREPARED BY SPRAY PYROLYSIS

Michael H. Jin[1,3], Kulinder K. Banger[1,3], Jerry D. Harris[2,3], and Aloysius F. Hepp[3]
[1]Ohio Aerospace Institute, Brookpark, OH 44142, USA
[2]Department of Chemistry, Cleveland State University, Cleveland, OH 44115, USA
[3]NASA Glenn Research Center, Cleveland, OH 44135, USA

ABSTRACT

Ternary single-source precursors were used to deposit CuInS$_2$ thin films using chemical spray pyrolysis. We investigated the effect of the film composition on texture, secondary phase formation, and grain size. As-grown films were most often In-rich. They became more (204/220)-oriented as indium concentration increased, and always contained a yet unidentified secondary phase. The (112)-preferred orientation became more pronounced as the film composition became more Cu-rich. The secondary phase was determined to be an In-rich compound based on composition analysis and Raman spectroscopy. In addition, as-grown Cu-rich (112)-oriented films did not exhibit the In-rich compound. Depositing a thin Cu layer prior to the growth of CuInS$_2$ increased the maximum grain size from ~ 0.5 μm to ~ 1 μm, and prevented the formation of the In-rich secondary phase.

1. INTRODUCTION

Thin film polycrystalline materials have been studied extensively for solar cell applications partially because their polycrystalline nature allows their formation on many different types of substrates [1]. Using lightweight polymer substrates for solar cells will particularly benefit space missions by reducing the power requirement for launching spacecraft [2]. Previously we have developed new single-source precursors (SSPs) for chalcopyrite thin film deposition [3-5], and successfully showed that SSPs' thermal properties were appropriate for low-temperature processes.

CuInS$_2$ is a wide band gap chalcopyrite and a promising material for thin film solar cells because of its near optimum direct band gap of 1.5 eV and its possible use as a top cell in a tandem structure with Cu(In,Ga)Se$_2$ (CIGS) [6]. While the best thin film solar cell efficiency reported was set by a CIGS heterojunction cell (~ 19 %) made at the National Renewable Energy Laboratory (NREL), CuInS$_2$ solar cells are theoretically expected to show efficiencies superior to those of CIGS cells [7]. However, a total area efficiency of only 11.4 % has been achieved so far for CuInS$_2$ cells [8].

Although those world-record cells were made with an In-rich CIGS and a Cu-rich CuInS$_2$ respectively, it has been well accepted that a Cu-rich stage during the film growth is necessary for both materials to achieve a large, columnar grain structure required for high performance solar cells. It is believed that the quasi-liquid Cu-Se (or S) binary phase segregated at the film surface, enhances the mobility of Cu and Se (or S) atoms during film growth [9].

While large grain growth requires a Cu-rich stage, an In-rich surface is also important because In-rich composition creates shallow donor states at the surface, and they result in Fermi level pinning and subsequent type inversion from p to n [6]. This surface inversion is believed to minimize recombination losses at the interface of the heterojunction during cell operation [10]. Therefore, an overall In-rich composition of CIGS is typically realized by having a final In-rich growth stage.

In contrast to CIGS, the best CuInS$_2$ cell reported was made using a Cu-rich layer without an intentionally made In-rich surface [8], even though the same advantage from the In-rich surface was expected. Surprisingly, forming the desirable In-rich surface layer has not been easy for CuInS$_2$ [6,11,12].

Because of the significance of systematic control of the composition during CuInS$_2$ film growth, we studied the composition of CuInS$_2$ films deposited using SSPs, and its effect on film texture, secondary phase formation, and grain structure.

2. EXPERIMENTAL

CuInS$_2$ SSPs, [(PPh$_3$)$_2$CuIn(SEt)$_4$] (solid) , [{P(n-Bu)$_3$}$_2$CuIn(SEt)$_4$] (liquid), and [{P(n-Bu)$_3$}$_2$CuIn(SPr^n)$_4$] (liquid) were synthesized following a procedure reported previously [3]. Aerosol-assisted chemical vapor deposition (AACVD) - or so-called 'chemical spray pyrolysis', was performed in four different AACVD reactors. The first reactor is a horizontal atmospheric pressure hot-wall reactor (reactor A) with a plate-type ultrasonic nebulizer (Sonaer Ultrasonics, 2.5 MHz). The second reactor is a vertical atmospheric pressure cold-wall reactor (reactor B) with a commercial ultrasonic nozzle (Sono-Tek, 120 kHz), and the third is a horizontal low-pressure hot-wall reactor (reactor C) with a pulsed aerosol injection system. A detailed film growth process with schematics of the reactors can be found elsewhere for reactors A, B, and C [4,5]. The fourth reactor (fig. 1) is a vertical atmospheric pressure hot-wall reactor (reactor D) with a commercial ultrasonic nozzle (Sono-Tek, 120 kHz).

Films were deposited at substrate temperatures from 350 °C to 450 °C, and either glass slides (Corning 2947 and 7059) or molybdenum (foil and Mo-coated glass slides) were typically used as the substrate. The description of the deposition processes for five representative films (I, II, III, IV, and V) is summarized elsewhere [13].

Three Cu-coated glass substrates were prepared using an evaporator (Varian) to study secondary phase formation and grain size of CuInS$_2$ subsequently grown on top. The

thickness of the Cu layer is about 50 nm, and three CuInS$_2$ films (#1, #2 and #3) were deposited using either reactor C or D (Table I).

Film thickness was measured by a profilometer (KLA-Tencor HRP 75), and X-ray diffraction (XRD) and glancing angle XRD (GAXRD) (Philips) were performed for phase identification. Film morphology was examined using scanning electron microscopes (Hitachi S-3000N and S-800), and the composition of the films was analyzed by energy dispersive spectroscopy (EDS) (EDAX). Further structural characterization was performed by Almega dispersive Raman spectroscopy (Thermo Nicolet).
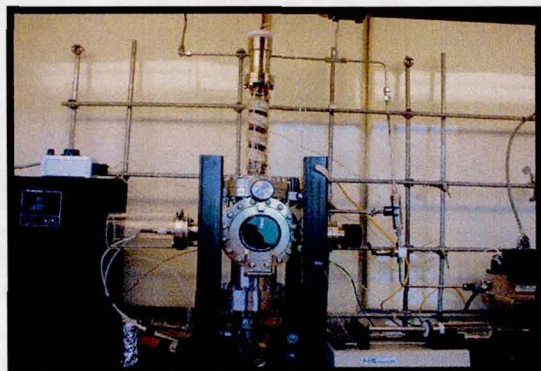

Fig. 1 Vertical atmospheric pressure hot-wall reactor (reactor D) built with a commercial ultrasonic nozzle (Sono-Tek, 120 kHz) and syringe-driven precursor solution delivery system.

Table I. CuInS$_2$ films deposited on both glass and Cu-coated glass simultaneously.

Film	#1	#2	#3
Reactor	C	C	D
Precursor	Pr[#]	Pr[#]	Et[*]
Substrate Temp. (°C)	350	400	350
Zone Temp. Zone 1 (°C)	70	106	Single hot zone
Zone 2 (°C)	70	70	120
Pr[#]: [{P(n-Bu)$_3$}$_2$CuIn(SPr^n)$_4$] (liquid) Et[*]: [{P(n-Bu)$_3$}$_2$CuIn(SEt)$_4$] (liquid)			

3. RESULTS AND DISCUSSION

Fig. 2 exhibits representative SEM pictures showing the grain morphology of films deposited in the three different reactors. Dense grain structure was realized with the hot-wall reactors. Fig. 2(a) shows an example of the columnar grain structure (Film I), which is desirable because photo-excited carriers can easily recombine at grain boundaries, and a vertical columnar grain structure can lower the cross section of recombination. In contrast, film III grown with the cold-wall reactor B showed a porous structure (fig. 2(b)). Due to the cold-wall configuration, the liquid precursor is only partially evaporated which can cause grain growth under liquid deposition instead of vapor deposition, yielding porous films [14]. This growth mechanism was recently discussed in great detail [5].

Films IV and V grown with reactor C had representative grain structures that we have often observed throughout this study. The dendritic microstructure (film IV, fig. 2(c)) exhibited non-faceted and elongated grains, which were also observed in films grown with solid SSPs in reactor A [4]. This was studied previously, and concluded to be a consequence of diffusion-limited growth [15]. By increasing the flow rate, dense and faceted trigonal-shaped grains were obtained (film V, fig. 2(d)). The intersection of {112} faces in the chalcopyrite structure creates the trigonal-shaped grains. Grain size for film V was about 0.5 μm, which is the largest grain size we have achieved thus far with as-grown films (~ 1 μm thick).

XRD patterns (fig. 3) showed that the films were either (112) or (204/220) preferentially oriented chalcopyrite structure. In addition, films often contained a secondary phase at 2θ ≈ 26.4° as shown in the XRD patterns. A diffraction peak located near the same 2θ position was previously observed when either In-rich or S-rich solutions were used for spray pyrolysis, and was identified as a C$_3$H$_4$Cl$_2$N$_6$ phase [16]. However, the C$_3$H$_4$Cl$_2$N$_6$ phase cannot be responsible for the peak observed in this study because SSPs do not produce by-products, which can form the phase. A recent study could not assign the same reflection at 26.5° to any single phase, but found that it was characteristic of In-rich films [17].
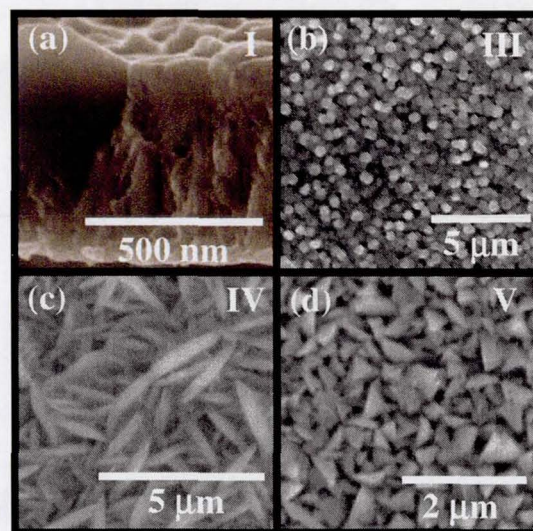

Fig. 2 SEM micrographs of CuInS2 films grown by aerosol-assisted chemical vapor deposition: (a) the cross-section image of film I, and (b) (c) (d) the plane-view images of films III, IV, and V respectively.

One constant observation in this study was the correlation of (204/220) film orientation and an In-rich stoichiometry and presence of a secondary phase (fig. 3). A previous study from our labs on SSPs showed this trend although it was not examined [5]. Contreras et al. reported that there is an equivalent symmetry between the {100} plane of γ-In$_2$Se$_3$ (hexagonal) and the {102} plane of CuInSe$_2$, and γ-In$_2$Se$_3$ can be a precursor layer of (204)-oriented CuInSe$_2$ [18]. While the secondary phase observed is not likely γ-In$_2$S$_3$ which does not have a diffraction peak at around 26.4°, it is conclusive that the secon-

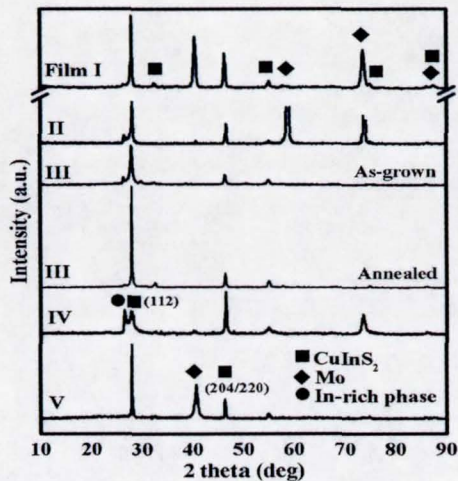dary phase is a result of an unidentified In-rich compound (either binary or ternary phase).

Fig. 3 XRD spectra of $CuInS_2$ films grown by aerosol-assisted chemical vapor deposition

EDS measurements (fig. 4) revealed films containing the secondary phase were always slightly In-rich, and an increase in the Cu/In ratio was observed when the secondary phase was removed by annealing at 600 °C for 15 min under a N_2 atmosphere (fig. 3). Ruckh et al. studied thermal decomposition of $CuInSe_2$ films up to 750 °C, and showed the desorption of In_2Se starting at 600 °C without losing any Cu-containing species [19].
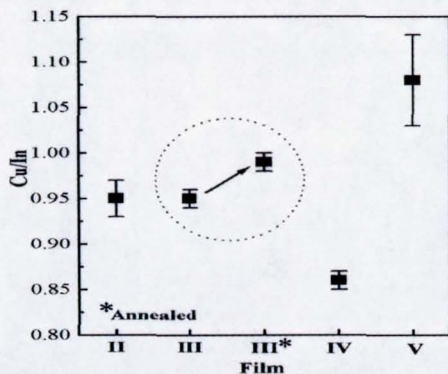

Fig. 4 Cu/In ratio of $CuInS_2$ films determined from electron dispersive spectroscopy.

The GAXRD pattern (fig. 5) shows that the secondary phase is more concentrated at the surface. Several films containing the secondary phase were etched in a 10 % aqueous KCN solution for 2 min, which is a typical etch recipe to remove a copper sulfide phase segregated to the surface of $CuInS_2$ [20]. The GAXRD patterns after etching (not shown) confirmed the secondary phase was not removed by the etch solution. If the secondary phase

was any type of a copper sulfide phase, it should have been easily etched away by the solution since the etch rate of Cu-rich phases in KCN solutions is much higher than that of In-rich phases [20].

In order to correlate further between the secondary phase and the In-rich environment, Raman spectroscopy was previously performed [13]. We observed that the spectrum showed a very strong mode at 305 cm^{-1} when the film was In-rich, (204/220)-oriented, and contained a significant amount of the secondary phase. However, the mode was least detectable for Cu-rich (112)-oriented films. It was reported that this additional mode could be assigned to a defect-related In-rich local vibrational mode [21], and the In-rich secondary phase could originate from this In-rich local environment. However, alternate ordering of Cu and In on the (201) planes of metal sublattice (called 'Cu-Au ordering') was found in polycrystalline $CuInS_2$ films [21], and this ordering could also be the origin of the mode. Further discussion about this mode can be found in the literature [21].
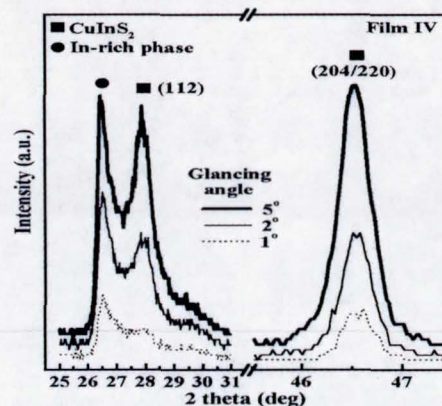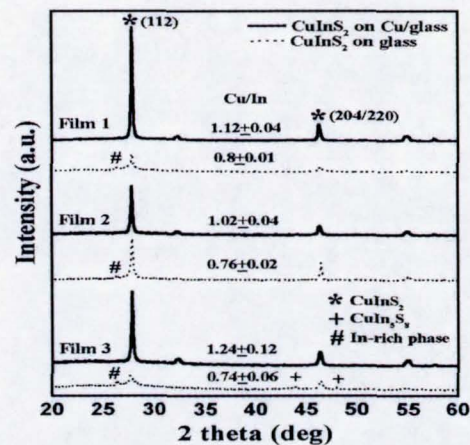

Fig. 5 GAXRD spetra of $CuInS_2$ film (IV).

Fig. 6 XRD patterns of CuInS2 films deposited on both glass and Cu-coated glass simultaneously.

Although as-grown Cu-rich films could be obtained without the Cu-precursor layer, their composition was only slightly Cu-rich, and grain size was less than 0.5 μm. In order to achieve larger grain growth and to investigate the identity of the secondary phase further, the 50 nm thick Cu-precursor layer was evaporated onto a part of a glass substrate before $CuInS_2$ deposition.

Fig. 6 shows that films on glass region were all In-rich and contained secondary In-rich phases. In contrast, films on the Cu layer were strongly (112)-oriented and did not contain any In-rich phase. This result also indicated that the unidentified phase is, in fact, an In-rich compound. SEM (fig. 7) exhibited the film (film #1) on the Cu layer had much larger grains (~ 1 μm) than the film on glass.
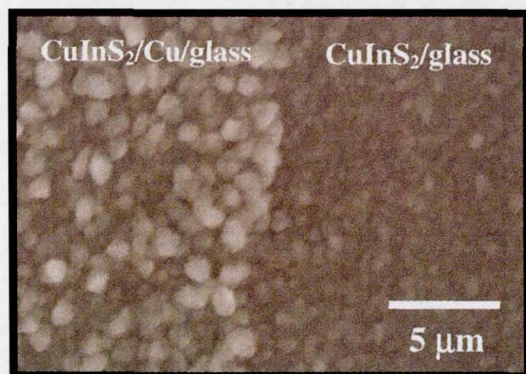

Fig. 7 SEM micrograph of $CuInS_2$ film deposited on both glass and Cu-coated glass simultaneously.

4. CONCLUSIONS

We have succeeded in depositing (112)-oriented films without a secondary phase using ternary SSPs in AACVD reactors. Meanwhile, it was not possible to grow In-rich (204/220)-oriented films without a secondary phase. The compositional nature of the secondary phase was studied using Raman spectroscopy, surface etching, thermal annealing and a Cu-precursor layer, and it is concluded to be an In-rich compound. Achieving larger grain size took precedence, and films grown on top of the Cu-precursor layer had larger grains than films deposited without the Cu-layer.

5. ACKNOWLEDGEMENT

REFERENCES

[1] F. Kessler, K. Herz, M. Powalla, M. Hartmann, M. Schmidt, A. Jasenek, and H. W. Schock, *Mat. Res. Soc. Symp. Proc.* **668**, H3.6.1 (2001).

[2] G. A. Landis and A. F. Hepp, *Proceedings of European Space Power Conference, ESA* **SP-320**, 517 (1991).

[3] K. K. Banger, J. Cowen, and A. F. Hepp, *Chem. Mater.* **13**, 3827 (2001).

[4] J. D. Harris, D. G. Hehemann, J. E. Cowen, A. F. Hepp, R. P. Raffaelle, and J. A. Hollingsworth, *Proceedings of the 28th Photovoltaic Specialists Conference*, (IEEE, Anchorage, 2000) p.563.

[5] M. H.-C. Jin, K. K. Banger, J. D. Harris, J. E. Cowen, and A. F. Hepp, *Proceedings of the 29th Photovoltaic Specialists Conference*, (IEEE, New Orleans, 2002) p.672.

[6] M. D. Archer and R. Hill, *Clean Electricity From Photovoltaics*, Chapter 7 (Imperial College Press, 2001).

[7] M. A. Contreras, B. Egaas, K. Ramanathan, J. Hiltner, A. Swartzlander, F. Hasoon, and R. Noufi, *Prog. Photovoltaic Res. Appl.* **7**, 311 (1999).

[8] K. Siemer, J. Klaer, I. Luck, J. Bruns, R. Klenk, and D. Bräunig, *Sol. Energy. Mater. Sol. Cells* **67**, 159 (2001).

[9] R. Klenk, T. Walter, H. W. Schock, and D. Cahen, *Adv. Mater.* **5**, 114 (1993).

[10] H. W. Schock and U. Rau, *Physica B* **308-310**, 1081 (2001).

[11] T. Walter and H. W. Schock, *Jpn. J. Appl. Phys.* **32-3**, 116 (1993).

[12] R. Scheer, M. Alt, I. Luck, H. J. Lewerenz, *Sol. Energy. Mater. Sol. Cells* **49**, 423 (1997).

[13] M. H.-C. Jin, K. K. Banger, J. D. Harris, J. E. Cowen, and A. F. Hepp, *Mat. Res. Soc. Symp. Proc.* **763**, B8.23.1 (to be published).

[14] T. T. Kodas and M. J. Hampden-Smith, *Aerosol Processing of Materials*, Chapter 5 (WILEY-VCH, 1999).

[15] J. A. Hollingsworth, A. F. Hepp, and W. E. Buhro, *Chem. Vap. Deposition* **5**, 105 (1999).

[16] M. Krunks, V. Mikli, O. Bijakina, H. Rebane, A. Mere, T. Varema, and E. Mellikov, *Thin Solid Films* **361-362**, 61 (2000).

[17] I. V. Luck, J. Alvarez-Garcia, L. Calvo-Barrio, A. Werner, A. Perez-Rodriguez, J. R. Morante, and D. Bräunig, *Mat. Res. Soc. Symp. Proc.* **668**, H1.4.1 (2001).

[18] M. A. Contreras, B. Egaas, D. King, A. Swartzlander, and T. Dullweber, *Thin Solid Films* **361-362**, 167 (2000).

[19] M. Ruckh, J. Kessler, T. A. Oberacker, and H. W. Schock, *Jpn. J. Appl. Phys.* **32-3**, 65 (1993).

[20] M. Weber, R. Scheer, H. J. Lewerenz, H. Jungblut, and U. Störkel, *J. Electrochem. Soc.* **149**, G77 (2002).

[21] D. S. Su, W. Neumann, and M. Giersig, *Thin Solid Films* **361-362**, 218 (2000).